Published in final edited form as:

Prostate. 2017 November ; 77(15): 1452–1467. doi:10.1002/pros.23400.

The Protein Kinase C Super-family Member PKN is Regulated by mTOR and Influences Differentiation During Prostate Cancer Progression

Chun-Song Yang[1], **Tiffany A. Melhuish**[1], **Adam Spencer**[1], **Li Ni**[1], **Yi Hao**[1], **Kasey Jividen**[1], **Thurl Harris**[2], **Chelsi Snow**[1], **Henry Frierson**[3], **David Wotton**[1,4], and **Bryce M. Paschal**[1,4,5]

[1]Center for Cell Signaling, University of Virginia, Charlottesville, VA, 22908, USA

[2]Department of Pharmacology, University of Virginia, Charlottesville, VA, 22908, USA

[3]Department of Pathology, University of Virginia, Charlottesville, VA, 22908, USA

[4]Department of Biochemistry and Molecular Genetics, University of Virginia, VA, 22908, USA

Abstract

Background—Phosphoinositide-3 (PI-3) kinase signaling has a pervasive role in cancer. One of the key effectors of PI-3 kinase signaling is AKT, a kinase that promotes growth and survival in a variety of cancers. Genetically engineered mouse models of prostate cancer have shown that AKT signaling is sufficient to induce prostatic epithelial neoplasia (PIN), but insufficient for progression to adenocarcinoma. This contrasts with the phenotype of mice with prostate-specific deletion of Pten, where excessive PI-3 kinase signaling induces both PIN and locally invasive carcinoma. We reasoned that additional PI-3 kinase effector kinases promote prostate cancer progression via activities that provide biological complementarity to AKT. We focused on the PKN kinase family members, which undergo activation in response to PI-3 kinase signaling, show expression changes in prostate cancer, and contribute to cell motility pathways in cancer cells.

Methods—PKN kinase activity was measured by incorporation of ^{32}P into protein substrates. Phosphorylation of the turn-motif (TM) in PKN proteins by mTOR was analyzed using the TORC2-specific inhibitor torin and a PKN1 phospho-TM-specific antibody. Amino acid substitutions in the TM of PKN were engineered and assayed for effects on kinase activity. Cell motility-related functions and PKN localization was analyzed by depletion approaches and immunofluorescence microscopy, respectively. The contribution of PKN proteins to prostate tumorigenesis was characterized in several mouse models that express PKN transgenes. The requirement for PKN activity in prostate cancer initiated by loss of phosphatase and tensin homologue deleted on chromosome 10 (Pten), and the potential redundancy between PKN isoforms, was analyzed by prostate-specific deletion of Pkn1, Pkn2, and Pten.

[5]corresponding author: Bryce M. Paschal, Center for Cell Signaling, Department of Biochemistry & Molecular Genetics, University of Virginia, Room 7021 West Complex, Box 800577, Health Sciences Center, 1400 Jefferson Park Avenue, Charlottesville, VA 22908-0577, paschal@virginia.edu, Office 434.243.6521, Lab 434.924.1532, Fax 434.924.1236.

Conflicts of Interest

The authors have no conflicts to disclose.

Results and Conclusions—PKN1 and PKN2 contribute to motility pathways in human prostate cancer cells. PKN1 and PKN2 kinase activity is regulated by TORC2-dependent phosphorylation of the TM, which together with published data indicates that PKN proteins receive multiple PI-3 kinase-dependent inputs. Transgenic expression of active AKT and PKN1 is not sufficient for progression beyond PIN. Moreover, Pkn1 is not required for tumorigenesis initiated by loss of Pten. Triple knockout of Pten, Pkn1, and Pkn2 in mouse prostate results in squamous cell carcinoma, an uncommon but therapy-resistant form of prostate cancer.

Keywords

phosphorylation; PI-3 kinase; mouse models; squamous cell carcinoma

INTRODUCTION

PI-3 kinases are a family of lipid and protein-modifying enzymes that regulate cellular functions including growth, proliferation, survival, and motility. Abnormal signaling by PI-3 kinases is common feature of a variety of cancers and occurs by multiple mechanisms. The most common mechanism is reduction or loss of PTEN, a tumor suppressor that negatively regulates PI-3 kinase by dephosphorylating the phosphorylated phosphatidyl inositol products. PTEN mutations and deletions occur in approximately 30% of primary human prostate tumors, and about 63% of metastatic tumors [1–4].

Genetically engineered mouse models have been developed to study how PI-3 kinase and PTEN contribute to cancer initiation and progression. The PTEN knockout is embryonic lethal [5], but hypomorphic alleles of PTEN and conditional mutants using Cre-lox have been used to formally demonstrate that PTEN functions as a tumor suppressor in multiple murine tissues including the prostate[6–9]. Conditional loss of Pten in mouse prostate results in PIN by about 6 weeks, and HGPIN by 8–9 weeks, with 100% penetrance. These mice develop focal invasion that progresses to wide spread locally invasive cancer in the majority of animals by 6–12 months [6, 10].

One of the major effectors of PI-3 kinase signaling that is robustly activated upon loss of PTEN is AKT/PKB. AKT activation is PI-3 kinase-activity sensitive because it contains a pleckstrin homology (PH) domain that binds phosphorylated phosphatidyl inositol generated at the plasma membrane. Once recruited to the plasma membrane, AKT is phosphorylated by 3-phosphoinositide-dependent kinase 1 (PDK1), which also contains a PH domain. Activated AKT contributes to tumorigenesis mostly through enhanced survival mechanisms, but also through increased proliferative and metabolic pathways [11]. A causal role for AKT in prostate cancer was examined by expressing myrisotylated AKT (myr-AKT; denoted active AKT) in mouse prostate[12, 13]. The myrisotylation tag drives AKT association with the plasma membrane resulting in its activation, even in WT cells. It was found that expression of active AKT is sufficient to generate highly penetrant PIN, but progression to adenocarcinoma and metastasis was not observed even after 78 weeks [10, 12, 13].

The fact that expression of activated AKT is not sufficient to phenocopy the effects of Pten loss in prostate indicates that additional effectors of PI-3 kinase signaling are likely required for prostate cancer progression beyond PIN. We hypothesized that the Ser/Thr kinase PKN1

[14] might fulfill the role of a PI-3 kinase effector that cooperates with AKT in prostate tumorigenesis. PKN1 is a member of the Protein Kinase C superfamily by virtue of sequence relatedness in the catalytic domain [15]. PKN1 and its paralogs PKN2 (59% identity) and PKN3 (55% identity) share biochemical properties with the PKC family, but also have unique forms of regulation. The later involves direct binding of Rho family GTPases to the N-terminus of PKN proteins, which relieves autoinhibition [16]. This feature is used to couple PKN activity to Rho-regulation of actin [17, 18]. PKN proteins and other PKC family members contain a hydrophobic docking motif for PDK1, the kinase responsible for activation loop phosphorylation [19]. PDK1 activity is critical for prostate tumorigenesis when Pten is deleted [20]. Additionally, PKN contains a short sequence near its C-terminus resembling the turn-motif (TM), which in other AGC kinases such as PKC and AKT is critical for enzyme stabilization[19]. mTORC2 mediates the phosphorylation of the TM of PKC and AKT [21].

These observations help place PKN proteins downstream of PI-3 kinase, PDK1, and mTOR, where we hypothesized it might cooperate with AKT to promote prostate tumorigenesis. We set out to explore this hypothesis using biochemical approaches and genetically engineered mouse models. Our data show that mTOR signaling has a dramatic effect on PKN kinase activity through phosphorylation of the TM. Using multiple mouse models, we found that PKN1 transgene expression has no discernable effect on prostate tumorigenesis in the context of active AKT, loss of Pten and expression of large T-antigen (TRAMP) [22]. However, deletion of Pkn1 together with its paralog Pkn2 in a background of Pten loss resulted in a squamous differentiation phenotype. Thus, when Pten is lost, PKN activity can contribute to the maintenance of a poorly differentiated (adenocarcinoma) phenotype during prostate tumorigenesis.

MATERIALS AND METHODS

Plasmids and siRNAs

PKN1 (Homo sapiens transcript variant 2, Origene, Rockville, MD, TC118456) and PKN2 (Addgene, Cambridge, MA, #20587) were cloned into pcDNA3 (Thermo Fisher Scientific, Grand Island, NY) along with an N-terminal Flag tag. PKN1 mutations of K644E, T774E, S916A, and N-terminal deletion of 1-568 amino acids (PKN1ΔN) were carried out by standard mutagenesis. The DNA fragment from AR (encoding residues 607–620) was cloned into pGex-4T vector (GE Healthcare Life Sciences, Pittsburgh, PA) to produce an N-terminal GST-fusion protein. For making stable cell lines, Flag-tagged PKN1 was cloned into the lentiviral vector pWPI (Addgene), which has a GFP expression marker for selection by flow cytometry, and into the puromycin-resistant plasmid pLH3. The pLH3 plasmid was generated from the pLKO.1puro shGFP (Addgene #12273) by replacing the hU6 promoter with a CMV promoter. For expression of transgenes in mice, PKN1 and PKN1ΔN genes were placed under the control of a prostate-specific probasin-promoter from the ARR_2Pb construct[23] (gift from Dr. Robert J. Matusik, Vanderbilt University). Other materials include constructs pGex-Marcks (96–184) (gift from Dr. Jae-Won Soh, Inha University) and lentiviral constructs and siRNAs for PKN knockdown (Sigma, St. Louis, MO, SHCLNG-NM_002741); siPKN1 (Thermo Fisher Scientific, Ambion siRNA ID 312, 314), siPKN2

(Thermo Fisher Scientific, Ambion siRNA ID 780, 781), and siRictor (GE-Dharmacon M-016984-02, Lafayette, CO).

Cell Culture and Transfection

293T cells were maintained and transfected in DMEM (Thermo Fisher Scientific) supplemented with 5% fetal bovine serum (FBS, Atlanta Biologicals, Flowery Branch, GA). Transient transfections were performed using the Fugene-6 protocol (Roche, Indianapolis, IN). PC3 and C4-2b cells (ATCC, Manassas, VA) were maintained and transfected in RPMI 1640 (Thermo Fisher Scientific) supplemented with 5% FBS, and transient transfections were performed using the TransFectin protocol (Bio-Rad, Hercules, CA). The siRNA transfections were done with Lipofectamine RNAiMax (Thermo Fisher Scientific) retro-transfection protocol. For lentivirus production, 293T cells were transfected with 1:1:2 ratio of pMD2g/psPAX2/target plasmid, incubated at 37°C for 16 h, switched to fresh DMEM supplemented with 30% FBS, and incubated for an additional 24 h. Virus-containing supernatants were transferred to sterile tubes, centrifuged at 2000 rpm, and supernatants passed through 0.45-μm filters to remove residual cells. Lentivirus infections were done on cells sparsely plated in 35-mm wells in the presence of 5–20% volume of virus supernatant diluted in fresh medium plus 8 μg/mL polybrene. Stably transfected cells were selected after two to three cell doublings by growth in the presence of 0.5−2 μg/mL of puromycin (Thermo Fisher Scientific), or isolated by flow cytometry based on GFP coexpression.

Antibodies

The antibodies used in this study included PKN1 (BD Biosciences, San Jose, CA, #610686, Santa Cruz, Dallas, TX, sc-1842), custom anti-PKN1 antibody (residues 105–115; cATHDGPQSPGA), PKN2 (BD Biosciences #610794, Epitomics, Cambridge, MA, #1498-1), phospho-PKN1(Thr774)/PKN2(Thr816) (Cell Signaling Technology, Danvers, MA, #2611), phospho-PKN1(Ser916) (custom-made against peptide CEAPTLpSPPRD), M2 (Sigma F3165), Histone H3 (Active Motif, Carlsbad, CA, #39163, Cell Signaling Technology #2650 and Abcam, Cambridge, MA, ab1791), phospho-H3(Thr6) (Abcam ab14102), phospho-H3(Ser10) (Active Motif #39253), phospho-H3(Thr11) (Cell Signaling Technology #9764 and Abcam ab5168), Phospho-Akt(Thr450) (Cell Signaling Technology #12178), Phospho-Akt(Ser473) (Cell Signaling Technology #4058), Akt (Cell Signaling Technology #9272), Phospho-PKCα/β II(Thr638/641) (Cell Signaling Technology #9375), PKC (Cell Signaling Technology #2056), E-Cadherin (Cell Signaling Technology #3195), Krt5 (Covance, Princeton, NJ, SIG-3475), Krt8 (Covance MMS-162P), Krt10 (Covance PRB-159P), and Ki67 (Abcam ab16667).

Kinase Assays

Flag-PKN1 and Flag-PKN2 were transiently transfected into 293T cells, with torin or rapamycin added 4 h before cell harvest at where indicated. Cells were lysed in a buffer containing 20 mM Tris-HCl, pH 7.5, 150 mM NaCl, 0.5% Triton X-100, 1 mM PMSF, 2 mM DTT, 5 mM EDTA, 5 μg/mL each of aprotinin/leupeptin/pepstatin, and 1:100 dilution of phosphatase inhibitor cocktail #1 and #2 (Roche). The cell extracts were incubated with M2-agarose (Sigma A2220) at 4°C for 4 h, and the beads were washed five times with the wash buffer carrying 20 mM Tris-HCl, pH 7.5, 150 mM NaCl, 0.1% Triton X-100, 1 mM

DTT, 0.1 mM EDTA, 1 μg/mL each of aprotinin/leupeptin/pepstatin, 2 mM sodium vanadate, and 0.4 μM Microcystin-LR (Enzo Life Sciences, Farmingdale, NY, Inc. #350-012-C100). The beads were either used directly in the kinase assays, or further eluted at room temperature with 20 μg/mL of Flag peptide in the wash buffer. The kinase assays were typically carried out at 30°C for 15–30 min in a 25 μL volume reaction of 50 mM Hepes, pH 7.0, 2 mM $MgCl^2$, 1 mg/mL BSA, 1 mM EGTA, 1 mM DTT, 0.1 mM ATP, 20 mM β-glycerophosphate, 0.15 mM sodium vanadate, 5 μg/mL each of aprotinin/leupeptin/pepstatin, 0.004% SDS, 2–5 μg substrate, the kinase, and 0.1 μL of γ-^{32}P-ATP. The reactions were stopped by the addition of SDS-PAGE loading buffer (1× final concentration).

Immunoblotting

Proteins were separated by SDS-PAGE and transferred to nitrocellulose membrane (Thermo Fisher Scientific). After standard incubations with blocking solution, primary antibody, and fluorescence-labeled secondary antibody (Alexa Fluor 680 donkey anti-rabbit IgG [H+L], Thermo Fisher Scientific A10043; or IRDye800 conjugated donkey anti-mouse IgG [H&L], Rockland, Limerick, PA, #610-732-124), proteins were detected and quantified on an Odyssey machine (LI-COR, Lincoln, NE).

Recombinant Proteins

GST-AR(607–620) and GST-Marcks were expressed in bacterial strain *BL21(DE3)pLysS* (EMD Millipore, Billerica, MA), and purified on glutathione beads using standard protocols.

Other Reagents

The other reagents included Torin (Thermo Fisher Scientific #424710), Rapamycin (Thermo Fisher Scientific #12-921), Histone H1 (EMD Chemicals, Gibbstown, NJ, #382150), Histone H3 (lab-made), ATP (Sigma A2383), γ-^{32}P-ATP (PerkinElmer, Waltham, MA), Flag peptide (Sigma F3290), M2-agarose (Sigma A2220), Puromycin (Thermo Fisher Scientific A11138-03), Hexadimethrine bromide (also named Polybrene, Sigma H9268), Fugene-6 (Promega, Madison, WI), TransFectin (Bio-Rad), Lipofectamine RNAiMax (Thermo Fisher Scientific).

Binucleate Measurements

These experiments were conducted as previously described [17].

Boyden chamber-based assays

The assays were performed in 24-well plates with 8.0-μm control inserts (Corning, Tewksbury, MA). The upper chamber was pretreated with either a low concentration of Matrigel (Sigma) for migration assays or a layer of Matrigel forming for invasion assays. Cells were seeded on the upper chamber of a trans-well chamber containing 0.5 mL of serum-free medium, and were allowed to migrate toward the lower chamber supplied with medium and 10% FBS. The cells were fixed in 4% formaldehyde and permeabilized in 0.2% Triton X-100. The cells at the top of the filter were removed with Q-tips, while the cells on

the other side of the filter were stained with DAPI. The migrating cells were examined and counted under a microscope for at least two experiments.

Gene Expression Analysis

Normalized gene expression data were obtained from the publicly available TCGA Data Portal. Using the PRAD dataset, comparisons between 52 prostate cancer (blue) and adjacent normal tissue (yellow) were represented via box and whisker plots. The expression values are calculated as "mRNA expression RNA-Seq by Expectation-Maximization (RSEM)," whiskers represent the minimum and maximum datapoints, and significance was determined using a paired t-test. The GSE6919 dataset[24] was downloaded for the following comparisons: normal (n = 63), prostate tumor (n = 65), and metastasis (n = 25). Significance was evaluated with an ANOVA combined with Tukey's multiple comparisons test.

Mice

Mouse embryonic injections were done in the Genetically Engineered Murine Model at the University of Virginia School of Medicine to obtain the prostate-specific transgene-expressing mice (PbPKN1^{+} and PbPKN1ΔN^{+}). Conditional alleles of *Pkn1* (UC Davis KOMP Repository, Davis, CA), *Pkn2* (UC Davis KOMP Repository), and *Pten* were combined with the *Pb-Cre4* [25] to drive prostate epithelium-specific deletion. The prostate-specific *caAKT1* transgene was obtained from the NCI MMHCC repository. Experimental animals were analyzed on a mixed C57BL/6 × FVB background. To combine the alleles, *Pten*$^{f/f}$ and *PbCre4* mice on a C57BL/6 background were crossed to PKN1$^{f/wt}$ and PKN2$^{f/wt}$ mice. These offspring were then intercrossed to generate the cohorts from which the experimental animals were generated. *Tg-Akt* or Tramp mice were crossed with PbPKN1^{+} or PbPKN1ΔN^{+}. *Tg-Akt* or Tramp mice were also crossed with *PbCre4 and PKN1*$^{f/f}$, and the experimental animals generated from intercrossing the offspring. All animal procedures were approved by the Animal Care and Use Committee at the University of Virginia, which is fully accredited by the AAALAC.

Histology, immunofluorescence, and whole mount imaging

Tissues were fixed in formalin, paraffin embedded, and sectioned at 5 microns, and were stained with hematoxylin and eosin (H&E), or prepared for immunostaining as previously described.[10, 26, 27] Images were captured on a Nikon Eclipse NI-U with a DS-QI1 or DS-Ri1 camera and NIS Elements software, and adjusted in Adobe Photoshop. Antibodies were as follows: rabbit anti-Krt10, chicken anti-Krt5, mouse anti-Krt8, and rabbit anti-Ki-67. Alexafluor 488, 546, and 647 secondary antibodies were from Thermo Fisher Scientific. Whole-mount *in situ hybridization* was performed on embryos with digoxigenin-labeled riboprobes, as described.[28] β-galactosidase staining was carried out as described[29]. Whole mount images were captured on a Leica MZ16 stereomicroscope and QImaging 5.0 RTV digital camera.

RESULTS

The carboxyl terminal region of AGC family members contains elements that are critical for regulating the structure and activity of the catalytic domain [19]. One of the elements that has been studied in detail is the turn motif (TM). In Akt and PKC, and other AGC family members, phosphorylation of the TM promotes stabilization and activity of the kinase through its contact with the amino-terminal small lobe (N-lobe) of the catalytic core. In this setting, the TM helps a second phosphorylated element, the hydrophobic motif (HM), wrap around the N-lobe and dock with the HM pocket [19].

The carboxyl terminal regions of PKN are 40–50% identical to PKC and Akt enzymes, and include sequences that are similar to the TM (see Fig. 2A). To assess whether the sequences resembling the TM in PKN proteins contribute to protein function, we introduced alanine substitutions into the predicted phospho-acceptor sites in the TM sequences of human PKN1 and PKN2. We then analyzed the kinase activity of WT and mutant proteins following expression in mammalian cells. Using Histone H3 as a substrate, PKN1 S916A and PKN2 T958A showed substantial reductions in kinase activity relative to the WT proteins (Fig. 1A).

TM phosphorylation in Akt and PKC enzymes is dependent on mTORC2 and occurs during protein translation.[21, 30] We applied the mTOR inhibitor Torin, which inhibits mTORC1 and mTORC2, to cells expressing WT PKN1 and PKN2 to test whether mTOR signaling is important for PKN kinase activity. PKN1 and PKN2 isolated from Torin-treated cells showed reduced phosphorylation of Histone H3, consistent with mTOR signaling to these kinases (Figure 1A). We reasoned this might involve phosphorylation of the TM of PKN1 and PKN2. To address this possibility, we studied the potential contribution of the TM in detail, focusing on PKN1. By quantitative analysis, PKN1 S916A showed a marked reduction in kinase activity towards four different substrates *in vitro*, including a site we mapped within the DNA-binding domain of the androgen receptor (Figure 1B; Supplemental Figure S1). Although Histone H3 showed the lowest level of phosphate incorporation in this assay, Thr11 in Histone H3 has been shown to be a PKN1 substrate.[31] We found that Histone H3 phosphorylation by PKN1 can occur on at least three sites, based on immunoblotting kinase reactions with Histone H3 phospho site-specific antibodies, and by probing cells transfected with constitutively active PKN1ΔN (Figure 1C). In a time course experiment with recombinant Histone H3 as the substrate, PKN1 S916A displayed very low levels of phosphorylation and auto-phosphorylation (Figure 1D). MARCKS is widely used as an *in vitro* PKC substrate. Increasing the concentration of MARCKS in the assay resulted in an increase in phosphate incorporation by the WT PKN1 but not by PKN1 S916A (Figure 1E). From these experiments, we conclude the TM makes a critical contribution to PKN kinase activity toward multiple substrates, and that PKN kinase activity can be regulated by mTOR.

Alignment of the TM sequences from human PKCα, PKNs, and AKT1 shows the putative phospho-acceptor site in PKN1 is a serine, while in the other kinases, this position is a threonine (Figure 2A). To determine if the TM of PKN1 is phosphorylated in cells, we generated an antibody to a peptide containing phospho-Ser916 and used it for probing

transfected PKN1. Antibody that was affinity-purified on the phospho-peptide recognized WT PKN1, and it displayed a low level of reactivity towards PKN S916A. Background reactivity was, however, eliminated when a low concentration of non-phosphorylated peptide was included in the antibody incubation (Figure 2B). PKN1 S916A was phosphorylated on T774 of the activation loop, indicating TM phosphorylation is not required for PDK1 phosphorylation of this site. TM phosphorylation was reduced in the activation loop mutant T774E and in the ATP-binding mutant K644E (Figure 2B), an indication that the TM might be sensitive to the catalytic core structure. Having determined that mTOR inhibition reduces the kinase activity of PKN (Figure 1), we used the antibody to examine whether Torin treatment affects TM phosphorylation. Indeed, treating cells with Torin caused a striking reduction in TM phosphorylation (Figure 2C). Rapamycin reduced but did not abolish PKN1 TM phosphorylation (Figure 2C). The complete loss of Ser916 phosphorylation by Torin treatment, together with the partial effect by Rapamycin, suggests that mTORC2 is largely, if not, solely responsible for TM phosphorylation in PKN1. Depletion of TORC2 components is known to reduce TM phosphorylation in Akt and PKC.[21, 32, 33]

To gain more insight into PKN1 TM phosphorylation, we examined the level of Ser916 phosphorylation after treating 293T cells with a range of Torin and Rapamycin concentrations (24 hrs). For comparison, we monitored TM phosphorylation in Akt and PKCα, since the TM within each of these kinases is phosphorylated by mTORC2 [21]. PKN1 showed a Torin-responsive reduction in TM that was similar to the reduction in Akt1 and PKCα (Fig. 3A). Under these conditions, TM phosphorylation was unaffected by rapamycin in all three kinases, which together with the Torin-sensitivity is consistent with phosphorylation by mTORC2. We then applied a relatively high concentration of Torin (250 nM) and examined site-specific phosphorylation in the three kinases. There was a very slight decline in PKN1 TM phosphorylation over 24 hrs, and minimal change in PKCα TM phosphorylation (Fig. 3B). Akt1 TM phosphorylation was also reduced over time, while the HM in Akt1 was dephosphorylated within approximately 30 min (Fig. 3B), indicating this site is more susceptible to phosphatase action than the TM in PKN1 and PKCα. Together, these data are consistent with mTORC2 phosphorylation of the TM in PKN1.

One of the functions previously ascribed to PKN proteins is modulation of actin dynamics, including contributions to cytokinesis in HeLa cells, and metastasis in PC-3 and DU145 prostate cells.[17, 34–36] To examine the contribution of PKN to cell motility in prostate cancer, we performed our analysis in C4-2b cells which, like PC-3 and DU145 cells, display robust motility characteristics in culture. We first used C4-2b cells stably transduced with FLAG-tagged PKN1 for immunolocalization experiments. We found that PKN1 stains small puncta in the cytoplasm of interphase cells, but during early anaphase becomes concentrated at the plasma membrane. PKN1 concentration likely reflects its early recruitment to the site of cleavage furrow formation, based on its nearly exclusive localization during cytokinesis (Figure 4A). This is very similar if not identical to the localization of PKN2 during cell division in HeLa cells.[17] Localization to the cleavage furrow suggested a possible role of PKN in cytokinesis in prostate cancer cells. We tested this possibility by scoring the effect of siRNA-mediated knockdown of PKN1 and PKN2 on successful completion of cytokinesis in C4-2b cells. Knockdown of PKN1 and PKN2 (alone and in combination) resulted in approximately 2% binucleate C4-2b cells in culture, which occurs as a consequence of

cytokinesis failure (Figures 4B–D). We next used Boyden chamber assays to assess PKN1 function in the migration in these cells. Stable overexpression of PKN1 approximately doubled C4-2b migration while knockdown of PKN1 using two different shRNAs reduced migration (Figures 4E and 4F). Transient knockdown of PKN1 and PKN2 cells reduced cell invasion through matrigel to about the same extent as knockdown of the mTORC2 subunit Rictor and treatment with Torin (Figure 4G). From these experiments, we conclude PKN1 and PKN2 are important for cell motility in prostate cancer cells, which has been established for PKN3 in PC-3 cells.[37]

PKN1 expression is higher in multiple cancers, including ovary, breast, and prostate.[38] PKN1 increases with Gleason score and modulates AR-dependent gene expression through Histone H3 phosphorylation.[31, 39] We used a PKN1 monoclonal antibody to stain a cohort of normal, primary, and metastatic prostate cancers. We found that PKN1 expression is increased in primary tumors, and undergoes a further increase in metastatic sites (Figures 5A and 5B). TCGA data (RNAseq) revealed that PKN1 expression is increased in prostate cancer (52 normal, 52 cancer), while PKN2 and PKN3 underwent a slight reduction in expression (Figure 5C). Akt expression was increased in tumor samples while PKCα was decreased (Figure 5C), the latter consistent with a tumor suppressor function.[40] mTOR catalytic subunit expression in this data set is higher in prostate tumors, consistent with immunocytochemical results from prostate tissue arrays,[41] though the scaffolding subunits RICTOR and RAPTOR appear unchanged. These and previously published data on PKN1 underscore the association between PKN1 expression with prostate cancer. Moreover, they show that the kinase responsible for TM phosphorylation (mTOR) and PKN activity is increased in tumor versus normal prostate cells (Figure 5C).

Pkn2 is required for embryonic development

To understand the roles of PKN function *in vivo*, we obtained mouse ES cells with targeted alleles of *Pkn1* and *Pkn2*. These alleles were created by KOMP as knock-out first alleles that can be converted to conditional alleles in which an essential exon is flanked by loxP sites (see Supplemental Fig. 2). Mice were generated from the two ES cell lines by standard procedures and germ-line transmission of each of the two *Pkn* alleles verified by PCR. For simplicity, we have termed the original KOMP knock-out first alleles ‘k’, the conditional alleles ‘f’ (for loxP flanked), and the Cre recombined, ‘r’. We first analyzed mice with the k alleles of either *Pkn1* or *Pkn2* for viability and fertility. As shown in Table 1, intercrossing $Pkn1^{+/k}$ heterozygotes generated $Pkn1^{k/k}$ mice at approximately the expected frequency in either a mixed strain background (C57BL6/N × 129Sv/J), or in a pure C57BL6/N background. In addition to being viable, $Pkn1^{k/k}$ mice bred successfully. In contrast to the *Pkn1* mutation, mice with homozygous $Pkn2^{k/k}$ alleles were not recovered at weaning, although $Pkn2^{+/k}$ heterozygotes appeared to be normal, and were obtained at the expected frequency from $Pkn2^{+/k}$ heterozygous intercrosses and from $Pkn2^{+/k}$ by wild type crosses (Table 1). We also observed a lack of homozygous *Pkn2* mutant animals when $Pkn2^{+/r}$ mice were intercrossed, suggesting that the Cre recombined allele was also a null. Mice that were doubly heterozygous for both *Pkn1* and *Pkn2* were viable and appeared grossly normal. When we intercrossed these double heterozygotes all genotypes were observed at the expected frequency at weaning, except for $Pkn2^{k/k}$ homozygotes, suggesting that there was

not a synthetic effect of deleting one *Pkn2* allele on top of both *Pkn1* alleles, for example (Table 2). Analyzing the genotypes for each gene separately from these crosses further emphasized the lack of genetic interaction, at least as far as overall viability is concerned.

In addition to generating a conditional loxP flanked allele by Flp-mediated recombination, we created lacZ reporter alleles (termed $Pkn1^{+/z}$ and $Pkn^{2+/z}$) for both *Pkn1* and *Pkn2* by first introducing a Cre recombinase (see Supplemental Figure S2). At embryonic day 10.5 (E10.5), we observed minimal staining for the lacZ reporter in $Pkn1^{+/z}$ embryos, whereas by E11.5, staining was evident in neural tissue, somites, limb buds, pharyngeal pouches, and the ventral region of the forebrain (Figure 6A). In contrast to *Pkn1*, *Pkn2* expression was evident from E6.5 to E9.5 and *Pkn2* appeared to be expressed widely throughout the embryo at all stages examined (Figure 6A). To determine when during development *Pkn2* null embryos failed, we generated litters of embryos from $Pkn2^{+/k}$ intercrosses at E7.5-E12.5. At E7.5-E10.5, $Pkn2^{k/k}$ homozygous embryos were identified, but all were clearly defective or severely delayed as compared to littermate controls (Table 3). Representative examples of $Pkn2^{k/k}$ homozygotes are shown (Figure 6B). By E7.5, the formation of the well-defined embryonic layers is delayed. In the *Pkn2* null embryos that were observable at E10.5, there was formation of the body axis, and specification of head and other major structures had initiated (Figure 6B). However, axial extension was clearly reduced and the embryos have not fully turned. To further examine axis formation, we examined control and *Pkn2* null embryos at E7.5 by whole mount *in situ* hybridization. Expression of the anterior neural marker, *Otx2* appeared to be relatively normal in *Pkn2* nulls, and *Brachyury* expression was also observed on the side of the embryo that was morphologically consistent with being the posterior (Figure 6C). This suggests that *Pkn2* null embryos specify the anterior-posterior axis and initiate the formation of neural tissue and posterior mesoderm, but fail to fully extend the axis and fail to progress to organogenesis. This is in agreement with a previous report detailing embryonic lethality and mesenchyme defects in Pkn2 null embryos.[42]

Analysis of Pkn function in prostate tumorigenesis

To explore the potential role of PKN proteins in prostate cancer progression, we took advantage of three genetically engineered mouse models that have been well characterized and recapitulate features of human prostate cancer.[43] Our major focus was PI-3 kinase signaling, since deletions and mutations in PI-3 kinase pathway components are common in prostate cancer. We made use of the Pten model of prostate cancer since conditional deletion of Pten in mouse prostate induces high-grade prostate intraepithelial neoplasia (HGPIN) by 8–9 weeks and locally invasive cancer by 6–12 months.[6, 10, 44] The second model we used is based on a transgenic mouse expressing constitutively active AKT (caAKT), which develops HGPIN but does not become invasive.[10, 12] The third model we used was TRAMP, which expresses Large T and small t antigens and develops HGPIN by 10–12 weeks of age.[45] The overall strategy was to test whether transgenic expression of PKN1 would enhance tumorigenic phenotypes, and whether PKN deletion would reduce tumorigenesis in these models.

Published studies have indicated that PKN expression is increased in human prostate cancer.[38, 39] To test if altered Pkn1 expression could contribute to prostate tumor formation or

progression in a mouse model, we first generated two lines of transgenic mice in which human PKN1 was expressed from a modified probasin (Pb) promoter that drives prostate epithelium-specific expression.[23] In one line, this promoter was linked to full length wild-type *PKN1* (*Tg-PKN1*), and in the other, we expressed an amino-terminally truncated version of PKN1 that is constitutively active (*Tg-PKN1ΔN*) (Figure 7A). Mice expressing either of these transgenes were normal and fertile, and even after 1 year of age, we observed no effects of transgene expression in the prostate (Figure 7B; Supplemental Figure S3A). Duct morphology appeared indistinguishable from that seen in wild-type mice and we detected no signs of dysplasia in the transgenic animals. Expression of *AKT1* from the probasin promoter has been shown to cause hyperplasia and low-grade PIN (prostate intra-epithelial neoplasia) that progresses to invasive cancer rarely, and generally only after more than 1 year of age. In our previous analyses, we observed phenotypes in ventral prostate of ~85% of *Tg-AKT1* mice, consistent with earlier reports.[10] When we compared the phenotype of *Tg-AKT1* mice to those with both the *Tg-AKT1* and one or other *PKN1* transgene, we did not observe any advancement of the AKT1-mediated PIN phenotype to invasive cancer even by more than 1 year of age (Figure 7C; Supplemental Figure S3B and Table 4). The frequency of mice with PIN was similar and we observed no change in either the later high-grade PIN (HGPIN) or in the *Tg-AKT1* PIN phenotype at onset. We next preformed a similar analysis by combining the PKN1 transgenes with a second oncogene-driven prostate cancer model (TRAMP), in which tumorigenesis is driven by prostate-specific expression of the SV40 large T antigen.[22] TRAMP mice develop HGPIN that progresses to invasive cancer with a neuroendocrine phenotype by around 20–25 weeks of age. As with the *Tg-AKT1* model, expression of *PKN1* in the TRAMP mice failed to alter the progression to HGPIN and invasive cancer (Figures 7D and 7E; Supplemental Figures S3C and S3D; and Table 4).

Conditional prostate-specific deletion of the *Pten* tumor suppressor has been one of the more widely used mouse models for prostate cancer.[43] Homozygous *Pten* deletion results in the development of PIN in all mice by around 6–8 weeks of age; the phenotype progresses rapidly to HGPIN and eventually to invasive cancer.[3, 6–8] We first tested for effects of human PKN1 overexpression in the background of the *Pten* null prostate tumor model. Comparison of *Pten* null tumors with *Pten* null tumors expressing a *PKN1* transgene did not reveal any differences in the type or severity of the tumors at any age examined (Figures 8A and 8B; Supplemental Figures S4A and S4B; and Table 4). Because expression of a *PKN1* transgene failed to alter tumor progression in mouse models of prostate cancer, we set out to test if loss of PKN affected tumorigenesis. Deletion of *Pkn1* alone in the context of a *Pten* null prostate did not affect tumor progression, at either the early PIN to HGPIN stages or later when a proportion of *Pten* null tumors become locally invasive (Table 4). Similarly, comparing the phenotypes in ventral prostate between *Pten* null and *Pten* null tumors lacking both *Pkn1* and *Pkn2* did not reveal any consistent differences (Figure 8C; Supplemental Figure S4C; and Table 4). However, in mice that had reached 45–60 weeks of age, we noticed the occurrence of extensive squamous differentiation, primarily in the anterior and dorsolateral lobes in three of four $Pten^{r/r};Pkn1^{r/r};Pkn2^{r/r}$ mice at ~53 weeks (Figure 8D; Supplemental Figure S4D; and Table 4). Squamous differentiation was not observed in any lobes from *Pten* null tumors from 18 mice at 45–60 weeks of age, suggesting this is linked to

the loss of Pkn proteins. To further examine the squamous phenotype, we stained *Pten*$^{r/r}$;*Pkn1*$^{r/r}$;*Pkn2*$^{r/r}$ tumors for the basal and luminal keratins, Krt5 and Krt8, as well as Krt10, which is indicative of squamous differentiation.[44] We observed strong expression of Krt10 and Krt5 in the tumors with squamous differentiation, that was distinct from regions of luminal cells marked by Krt8 expression (Figure 9A). Since we observed relatively large regions of squamous differentiation, we stained *Pten*$^{r/r}$;*Pkn1*$^{r/r}$;*Pkn2*$^{r/r}$ tumors for Krt5 and Krt8, together with Ki-67 to identify proliferating cells. The extent of proliferation was low in luminal regions and in basal cells surrounding intact HGPIN-positive ducts. By contrast, in regions where squamous differentiation was more pronounced, the proportion of proliferating cells was significantly higher (Figures 9B and 9C). Taken together, this suggests that loss of Pkn1 and Pkn2 in the context of a *Pten* null tumor results in increased proliferation with differentiation to a squamous phenotype.

DISCUSSION

PKN1 was originally discovered in screens for new PKC isoforms.[14, 46, 47] Our group's interest in PKN1 began with the finding that it is expressed in the 10 most common lethal carcinomas.[38] By IHC, PKN1 expression was highest in ovary, but the levels of PKN1 in prostate cancer were notable because the levels detected in normal prostate were very low. Other laboratories have reported that based on IHC analysis, PKN1 expression increases with Gleason score.[31] This is consistent with our IHC analysis showing that primary tumors and metastases have higher levels of PKN1. Based on microarray data,[24] PKN1 expression is increased in primary prostate tumors, and displays a further increase in expression in metastatic tumors. Similarly, RNA-seq data from TCGA show increased levels of PKN1 in prostate tumors relative to adjacent normal tissue. PKN2 and PKN3 do not show increased expression in primary prostate tumors, though microarray data suggest PKN2 levels are higher in metastases. All three forms of PKN can be detected in cancer cell lines derived from various tissue types (including prostate cancer), though the relative amounts of the three isoforms vary depending on the cancer cell line. For example, PKN1 protein levels are similar in LNCaP and C4-2b (unpublished observations) and lower in PC-3 cells.[48]

The aforementioned expression data represented part of the premise for exploring PKN1 as a key component in prostate cancer. More specifically, we viewed PKN1 as a candidate that cooperates with AKT during prostate tumorigenesis initiated by loss of Pten. The rationale for this viewpoint was based on several key observations: (i) activated AKT does not phenocopy loss of Pten,[12] which strongly implicates additional effectors of PI-3 kinase signaling in tumorigenesis; (ii) Pkn1 is directly phosphorylated by PDK1,[49] a PI-3 kinase effector kinase; (iii) Pkn1 kinase activity can be stimulated by phosphorylated lipids that are products of PI-3 kinase[50]; (iv) phosphorylation of the Pkn1 TM depends on TORC2 (this study), which is downstream of PI-3 kinase signaling; (v) the biological pathways associated with Pkn1 activity include regulation of the actin cytoskeleton,[36] which biologically can be considered as complementary to the growth and survival functions of AKT; (vi) Pkn1 physically associates with the androgen receptor and promotes transcription via reactions involving Histone H3 Thr11 phosphorylation.[31] These data, generated by multiple groups in the prostate cancer field over the past several years, provide robust support for a model of PI-3 kinase-dependent PKN activation in parallel with AKT activation. Our data showing

that PKN TM phosphorylation is critical for its ability to phosphorylate multiple substrates (Figure 1) suggest that mTOR function is fundamentally important for PKN activity. PKN proteins could be critical effectors of TORC2, which is known to regulate the actin cytoskeleton.[51]

Our analysis of embryonic phenotypes from Pkn mutant mice clearly shows an essential role for Pkn2, that cannot be compensated for by Pkn1 or Pkn3. RNA-seq analysis of E9.0 embryos suggests that Pkn2 is more highly expressed than Pkn1 or Pkn3,[26] and our analysis of lacZ reporter alleles for Pkn1 and Pkn2 confirms this view with Pkn2 showing widespread expression during early development. In agreement with previous work,[52] it appears that Pkn2 null embryos are developmentally delayed by E7.5, but do establish proximo-distal and anterior-posterior axes, suggesting that embryonic patterning is relatively normal. However, axis extension and embryo turning are defective, consistent with cell motility defects as seen *in vitro* with Pkn depletion.[48]

We used a panel of genetically engineered mouse models to rigorously examine the contributions of Pkn1 to prostate tumorigenesis. We explored our hypothesis that Pkn1 cooperates with Akt during PI-3 kinase-dependent prostate tumorigenesis using two strategies. The first strategy involved the expression of Pkn1 transgenes. Full-length PKN1 was co-expressed with active Akt with the goal of promoting disease progression beyond PIN. A related approach involved co-expressing a constitutively active form of PKN1 (PKN1ΔN) with active Akt. Neither combination promoted disease progression beyond the PIN phenotype attributable to Akt. We conclude from these experiments that activation of Pkn1 and Akt is insufficient to promote tumorigenesis beyond PIN. A caveat to this conclusion is the activity of endogenous Pkn1 and Akt in the setting of Pten loss might not be recapitulated by the transgenes, either in terms of expression level, sub-cellular distribution, or signaling output. Nonetheless, it seems probable that activation of these two kinases is insufficient for disease progression presumably because additional PI-3 kinase-regulated components are in play in the setting of Pten loss. We also introduced the Pkn1 transgenes into the TRAMP mouse. We observed no obvious effect on tumorigenesis, though it is possible that the strain background or cohort size limited our ability to detect subtle PKN transgene effect in this setting. We then considered the possibility that Pkn1 function and its biological effects in these models could be restrained by expression of Pten. Expression of Pkn1 in the background of Pten loss, however, had no obvious impact on turmorigenesis.

Our second strategy involved testing whether Pkn1 is necessary for prostate tumorigenesis, reasoning that Akt and Pkn1 activation are not sufficient for prostate tumorigenesis. To this end, we deleted both Pten and Pkn1 in prostate, but this combination did not yield any phenotype beyond that obtained by deleting Pten alone. From this result, we conclude that Pkn1 function is not required for tumorigenesis initiated by loss of Pten.

We considered whether the absence of a clear prostate cancer phenotype associated with Pkn1 might reflect the involvement of another Pkn isoform. While there may be some biochemical differences related to kinase regulation of the three Pkn proteins, all three enzymes have the same architecture, share closely related catalytic domains, and contribute

to functions associated with cell motility and actin cytoskeleton, including cell migration. Thus, we considered whether redundancy between the Pkn isoforms might occur. We focused our attention on Pkn2, which by RNA-seq shows much higher levels of expression (10 to 20-fold) relative to Pkn3 in the prostate cancer lines LNCaP and VCaP. The expression data from human prostate cancers (TCGA) shows a similar relationship. Moreover, Pkn1 and Pkn2 are expressed at much higher levels (20–40-fold) than Pkn3 in mouse prostate. Indeed, we found that depletion of either Pkn1 or Pkn2 was sufficient to generate cytokinesis defects and cell invasion defects in prostate cancer C4-2b cells.

We generated *Pten*$^{r/r}$;*Pkn1*$^{r/r}$;*Pkn2*$^{r/r}$ mice and examined the prostates for effects on tumorigenesis initiated by loss of Pten. Deletion of Pkn1 and Pkn2 did not alter the HGPIN or locally invasive phenotype caused simply by loss of Pten. However, in older mice (45–60 weeks of age) we determined there was a presence of squamous differentiation in the anterior and dorsolateral lobes 3 of 4 mice, as well as the ventral lobe of one of the same mice. This phenotype was not observed in *Pten* null tumors from 18 different mice of the same ages (45 to 60 weeks of age). This result suggests that Pkn1/Pkn2 activity helps restrain differentiation to a squamous phenotype. Because these cells are KRT5 positive and KRT8 negative, deletion of Pkn1/Pkn2 in the Pten null is likely promoting proliferation, and squamous differentiation of a basal cell population.

Squamous cell carcinoma of the prostate comprises ≤1% of all prostate cancers. While certain histological features including keratinization are characteristic of squamous differentiation in prostate cancer, the etiology is not defined. The prognosis for these patients is very poor for this therapy-resistant cancer, with survival times ranging from 1 to 13 months [53, 54]. Our data suggests that signaling through PKN might act as a restraint to squamous differentiation.

CONCLUSIONS

The kinase activity of PKN1 and PKN2 is regulated by TM phosphorylation mediated directly, or indirectly, by the TORC2 complex. PKN proteins contribute important cell motility functions in multiple cancer cell types, including prostate cancer. Pkn1 and Pkn2 function may be important for helping specify the differentiation state of prostate cancers that have lost the tumor suppressor Pten.

Supplementary Material

Refer to Web version on PubMed Central for supplementary material.

Acknowledgments

Funding Information

NCI #2P01CA104106 (BP and DW) and NINDS #NS077958 (DW)

References

1. McMenamin ME, et al. Loss of PTEN expression in paraffin-embedded primary prostate cancer correlates with high Gleason score and advanced stage. Cancer Res. 1999; 59(17):4291–6. [PubMed: 10485474]
2. Cairns P, et al. Frequent inactivation of PTEN/MMAC1 in primary prostate cancer. Cancer Res. 1997; 57(22):4997–5000. [PubMed: 9371490]
3. Suzuki H, et al. Interfocal heterogeneity of PTEN/MMAC1 gene alterations in multiple metastatic prostate cancer tissues. Cancer Res. 1998; 58(2):204–9. [PubMed: 9443392]
4. Wang SI, Parsons R, Ittmann M. Homozygous deletion of the PTEN tumor suppressor gene in a subset of prostate adenocarcinomas. Clin Cancer Res. 1998; 4(3):811–5. [PubMed: 9533551]
5. Di Cristofano A, et al. Pten is essential for embryonic development and tumour suppression. Nat Genet. 1998; 19(4):348–55. [PubMed: 9697695]
6. Trotman LC, et al. Pten dose dictates cancer progression in the prostate. PLoS Biol. 2003; 1(3):E59. [PubMed: 14691534]
7. Wang S, et al. Prostate-specific deletion of the murine Pten tumor suppressor gene leads to metastatic prostate cancer. Cancer Cell. 2003; 4(3):209–21. [PubMed: 14522255]
8. Ma X, et al. Targeted biallelic inactivation of Pten in the mouse prostate leads to prostate cancer accompanied by increased epithelial cell proliferation but not by reduced apoptosis. Cancer Res. 2005; 65(13):5730–9. [PubMed: 15994948]
9. Ratnacaram CK, et al. Temporally controlled ablation of PTEN in adult mouse prostate epithelium generates a model of invasive prostatic adenocarcinoma. Proc Natl Acad Sci U S A. 2008; 105(7): 2521–6. [PubMed: 18268330]
10. Bjerke GA, et al. Activation of Akt signaling in prostate induces a TGFbeta-mediated restraint on cancer progression and metastasis. Oncogene. 2014; 33(28):3660–7. [PubMed: 23995785]
11. Hennessy BT, et al. Exploiting the PI3K/AKT pathway for cancer drug discovery. Nat Rev Drug Discov. 2005; 4(12):988–1004. [PubMed: 16341064]
12. Majumder PK, et al. Prostate intraepithelial neoplasia induced by prostate restricted Akt activation: the MPAKT model. Proc Natl Acad Sci U S A. 2003; 100(13):7841–6. [PubMed: 12799464]
13. Li B, et al. Conditional Akt activation promotes androgen-independent progression of prostate cancer. Carcinogenesis. 2007; 28(3):572–83. [PubMed: 17032658]
14. Mukai H, et al. Activation of PKN, a novel 120-kDa protein kinase with leucine zipper-like sequences, by unsaturated fatty acids and by limited proteolysis. Biochem Biophys Res Commun. 1994; 204(1):348–56. [PubMed: 7945381]
15. Mellor H, Parker PJ. The extended protein kinase C superfamily. Biochem J. 1998; 332(Pt 2):281–92. [PubMed: 9601053]
16. Shibata H, et al. Characterization of the interaction between RhoA and the amino-terminal region of PKN. FEBS Lett. 1996; 385(3):221–4. [PubMed: 8647255]
17. Schmidt A, et al. Rho GTPases regulate PRK2/PKN2 to control entry into mitosis and exit from cytokinesis. EMBO J. 2007; 26(6):1624–36. [PubMed: 17332740]
18. Lim MA, et al. Roles of PDK-1 and PKN in regulating cell migration and cortical actin formation of PTEN-knockout cells. Oncogene. 2004; 23(58):9348–58. [PubMed: 15531926]
19. Pearce LR, Komander D, Alessi DR. The nuts and bolts of AGC protein kinases. Nat Rev Mol Cell Biol. 2010; 11(1):9–22. [PubMed: 20027184]
20. Bayascas JR, et al. Hypomorphic mutation of PDK1 suppresses tumorigenesis in PTEN(+/−) mice. Curr Biol. 2005; 15(20):1839–46. [PubMed: 16243031]
21. Ikenoue T, et al. Essential function of TORC2 in PKC and Akt turn motif phosphorylation, maturation and signalling. EMBO J. 2008; 27(14):1919–31. [PubMed: 18566587]
22. Greenberg NM, et al. Prostate cancer in a transgenic mouse. Proc Natl Acad Sci U S A. 1995; 92(8):3439–43. [PubMed: 7724580]
23. Zhang J, et al. A small composite probasin promoter confers high levels of prostate-specific gene expression through regulation by androgens and glucocorticoids in vitro and in vivo. Endocrinology. 2000; 141(12):4698–710. [PubMed: 11108285]

24. Yu YP, Landsittel D, Jing L, et al. Gene expression alterations in prostate cancer predicting tumor aggression and preceding development of malignancy. J Clin Oncol. 2004; 22(14):2790–2799. [PubMed: 15254046]
25. Wu X, Wu J, Huang J, et al. Generation of a prostate epithelial cell-specific Cre transgenic mouse model for tissue-specific gene ablation. Mech Dev. 2001; 101(1–2):61–69. [PubMed: 11231059]
26. Anderson AE, Taniguchi K, Hao Y, et al. Tgif1 and Tgif2 Repress Expression of the RabGAP Evi5l. Mol Cell Biol. 2017; 37(5)
27. Powers SE, Taniguchi K, Yen W, et al. Tgif1 and Tgif2 regulate Nodal signaling and are required for gastrulation. Development. 2010; 137(2):249–259. [PubMed: 20040491]
28. Melhuish TA, Taniguchi K, Wotton D. Tgif1 and Tgif2 Regulate Axial Patterning in Mouse. PLoS One. 2016; 11(5):e0155837. [PubMed: 27187787]
29. Nagy A, Gertsenstein M, Vintersten K, Behringer R. Staining Whole Mouse Embryos for {beta}-Galactosidase (lacZ) Activity. CSH Protoc. 2007; 2007 pdb prot4725.
30. Oh WJ, Wu CC, Kim SJ, et al. mTORC2 can associate with ribosomes to promote cotranslational phosphorylation and stability of nascent Akt polypeptide. EMBO J. 2010; 29(23):3939–3951. [PubMed: 21045808]
31. Metzger E, Yin N, Wissmann M, et al. Phosphorylation of histone H3 at threonine 11 establishes a novel chromatin mark for transcriptional regulation. Nat Cell Biol. 2008; 10(1):53–60. [PubMed: 18066052]
32. Hauge C, Antal TL, Hirschberg D, et al. Mechanism for activation of the growth factor-activated AGC kinases by turn motif phosphorylation. EMBO J. 2007; 26(9):2251–2261. [PubMed: 17446865]
33. Facchinetti V, Ouyang W, Wei H, et al. The mammalian target of rapamycin complex 2 controls folding and stability of Akt and protein kinase C. EMBO J. 2008; 27(14):1932–1943. [PubMed: 18566586]
34. Vincent S, Settleman J. The PRK2 kinase is a potential effector target of both Rho and Rac GTPases and regulates actin cytoskeletal organization. Mol Cell Biol. 1997; 17(4):2247–2256. [PubMed: 9121475]
35. Dong LQ, Landa LR, Wick MJ, et al. Phosphorylation of protein kinase N by phosphoinositide-dependent protein kinase-1 mediates insulin signals to the actin cytoskeleton. Proc Natl Acad Sci U S A. 2000; 97(10):5089–5094. [PubMed: 10792047]
36. Jilg CA, Ketscher A, Metzger E, et al. PRK1/PKN1 controls migration and metastasis of androgen-independent prostate cancer cells. Oncotarget. 2014; 5(24):12646–12664. [PubMed: 25504435]
37. Leenders F, Mopert K, Schmiedeknecht A, et al. PKN3 is required for malignant prostate cell growth downstream of activated PI 3-kinase. EMBO J. 2004; 23(16):3303–3313. [PubMed: 15282551]
38. Galgano MT, Conaway M, Spencer AM, Paschal BM, Frierson HF Jr. PRK1 distribution in normal tissues and carcinomas: overexpression and activation in ovarian serous carcinoma. Hum Pathol. 2009; 40(10):1434–1440. [PubMed: 19427017]
39. Metzger E, Muller JM, Ferrari S, Buettner R, Schule R. A novel inducible transactivation domain in the androgen receptor: implications for PRK in prostate cancer. EMBO J. 2003; 22(2):270–280. [PubMed: 12514133]
40. Antal CE, Hudson AM, Kang E, et al. Cancer-associated protein kinase C mutations reveal kinase's role as tumor suppressor. Cell. 2015; 160(3):489–502. [PubMed: 25619690]
41. Kremer CL, Klein RR, Mendelson J, et al. Expression of mTOR signaling pathway markers in prostate cancer progression. Prostate. 2006; 66(11):1203–1212. [PubMed: 16652388]
42. Quetier I, Marshall JJ, Spencer-Dene B, et al. Knockout of the PKN Family of Rho Effector Kinases Reveals a Non-redundant Role for PKN2 in Developmental Mesoderm Expansion. Cell Rep. 2016; 14(3):440–448. [PubMed: 26774483]
43. Irshad S, Abate-Shen C. Modeling prostate cancer in mice: something old, something new, something premalignant, something metastatic. Cancer Metastasis Rev. 2013; 32(1–2):109–122. [PubMed: 23114843]

44. Bjerke GA, Pietrzak K, Melhuish TA, Frierson HF Jr, Paschal BM, Wotton D. Prostate cancer induced by loss of Apc is restrained by TGFbeta signaling. PLoS One. 2014; 9(3):e92800. [PubMed: 24651496]
45. Gingrich JR, Barrios RJ, Kattan MW, Nahm HS, Finegold MJ, Greenberg NM. Androgen-independent prostate cancer progression in the TRAMP model. Cancer Res. 1997; 57(21):4687–4691. [PubMed: 9354422]
46. Morrice NA, Gabrielli B, Kemp BE, Wettenhall RE. A cardiolipin-activated protein kinase from rat liver structurally distinct from the protein kinases C. J Biol Chem. 1994; 269(31):20040–20046. [PubMed: 8051089]
47. Palmer RH, Ridden J, Parker PJ. Identification of multiple, novel, protein kinase C-related gene products. FEBS Lett. 1994; 356(1):5–8. [PubMed: 7988719]
48. Lachmann S, Jevons A, De Rycker M, et al. Regulatory domain selectivity in the cell-type specific PKN-dependence of cell migration. PLoS One. 2011; 6(7):e21732. [PubMed: 21754995]
49. Balendran A, Casamayor A, Deak M, et al. PDK1 acquires PDK2 activity in the presence of a synthetic peptide derived from the carboxyl terminus of PRK2. Curr Biol. 1999; 9(8):393–404. [PubMed: 10226025]
50. Palmer RH, Dekker LV, Woscholski R, Le Good JA, Gigg R, Parker PJ. Activation of PRK1 by phosphatidylinositol 4,5-bisphosphate and phosphatidylinositol 3,4,5-trisphosphate. A comparison with protein kinase C isotypes. J Biol Chem. 1995; 270(38):22412–22416. [PubMed: 7673228]
51. Jacinto E, Loewith R, Schmidt A, et al. Mammalian TOR complex 2 controls the actin cytoskeleton and is rapamycin insensitive. Nat Cell Biol. 2004; 6(11):1122–1128. [PubMed: 15467718]
52. Danno S, Kubouchi K, Mehruba M, et al. PKN2 is essential for mouse embryonic development and proliferation of mouse fibroblasts. Genes Cells. 2017; 22(2):220–236. [PubMed: 28102564]
53. Kanthan R, Torkian B. Squamous cell carcinoma of the prostate. A report of 6 cases. Urol Int. 2004; 72(1):28–31. [PubMed: 14730162]
54. Mohan H, Bal A, Punia RP, Bawa AS. Squamous cell carcinoma of the prostate. Int J Urol. 2003; 10(2):114–116. [PubMed: 12588611]

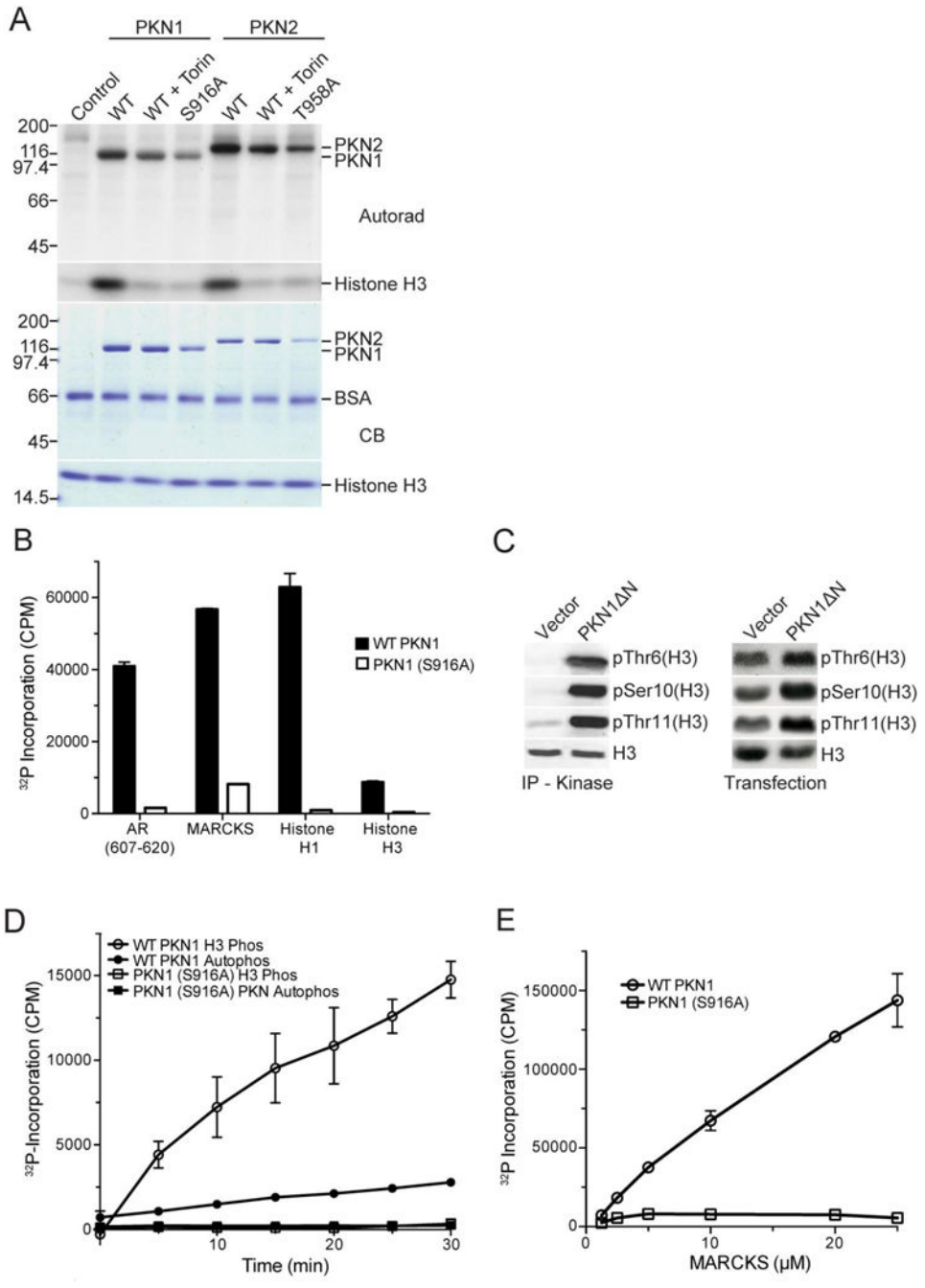

Fig. 1. Regulation of PKN kinase activity

IP-kinase assays with WT and TM mutants of PKN1 (S916A) and PKN2 (T958A). Torin inhibited the PKN kinase activity to about the same extent as mutating the TM in both PKN isoforms. (B) The PKN1 TM mutant S916A has reduced kinase activity towards multiple substrates. (C) Deletion of the PKN N-terminus results in constitutive histone H3 phosphorylation in vitro and in cells. (D, E) The PKN1 TM mutant S916A dramatically reduces autophosphorylation as well as Histone H3 and MARCKS phosphorylation.

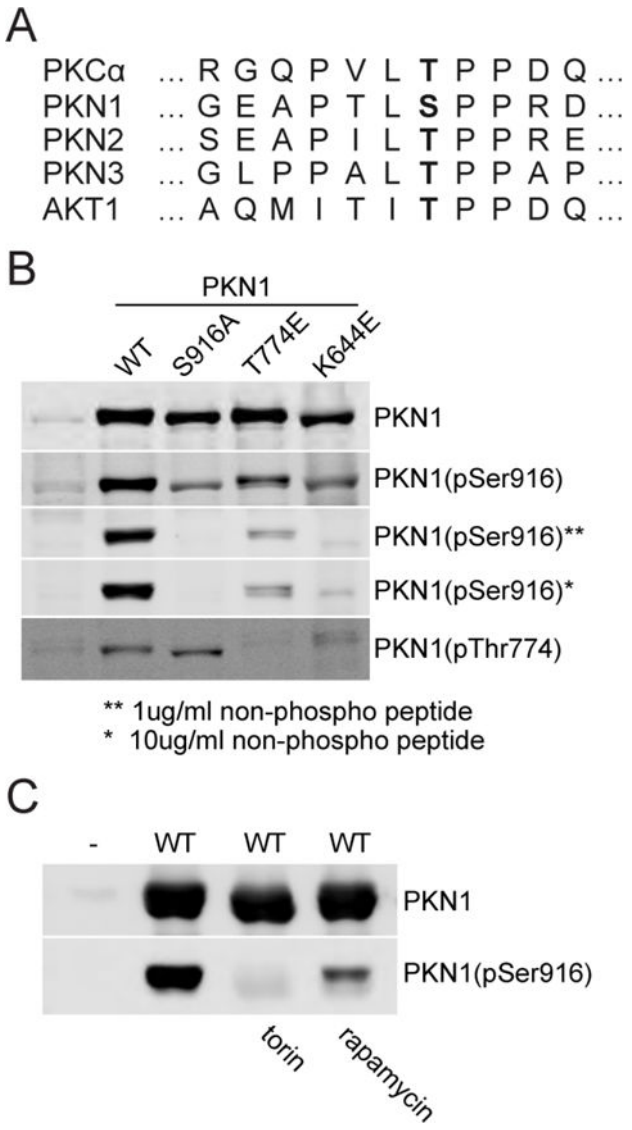

Fig. 2. PKN contains a TM phosphorylated by a torin-sensitive kinase

(A) Alignment of TM sequences with the predicted phosphorylated residues indicated (bold). (B) Transfection of PKN1 bearing mutations in the TM (S916A), activation loop (T774E) and ATP binding pocket (K644E) probed with antibodies specific for phos-S916 and phos-T774. Including non-phospho-TM peptide during the antibody incubation reduces the detection of non-phosphorylated PKN. (C) IP-blot of WT PKN1 expressed in cells treated with torin and rapamycin.

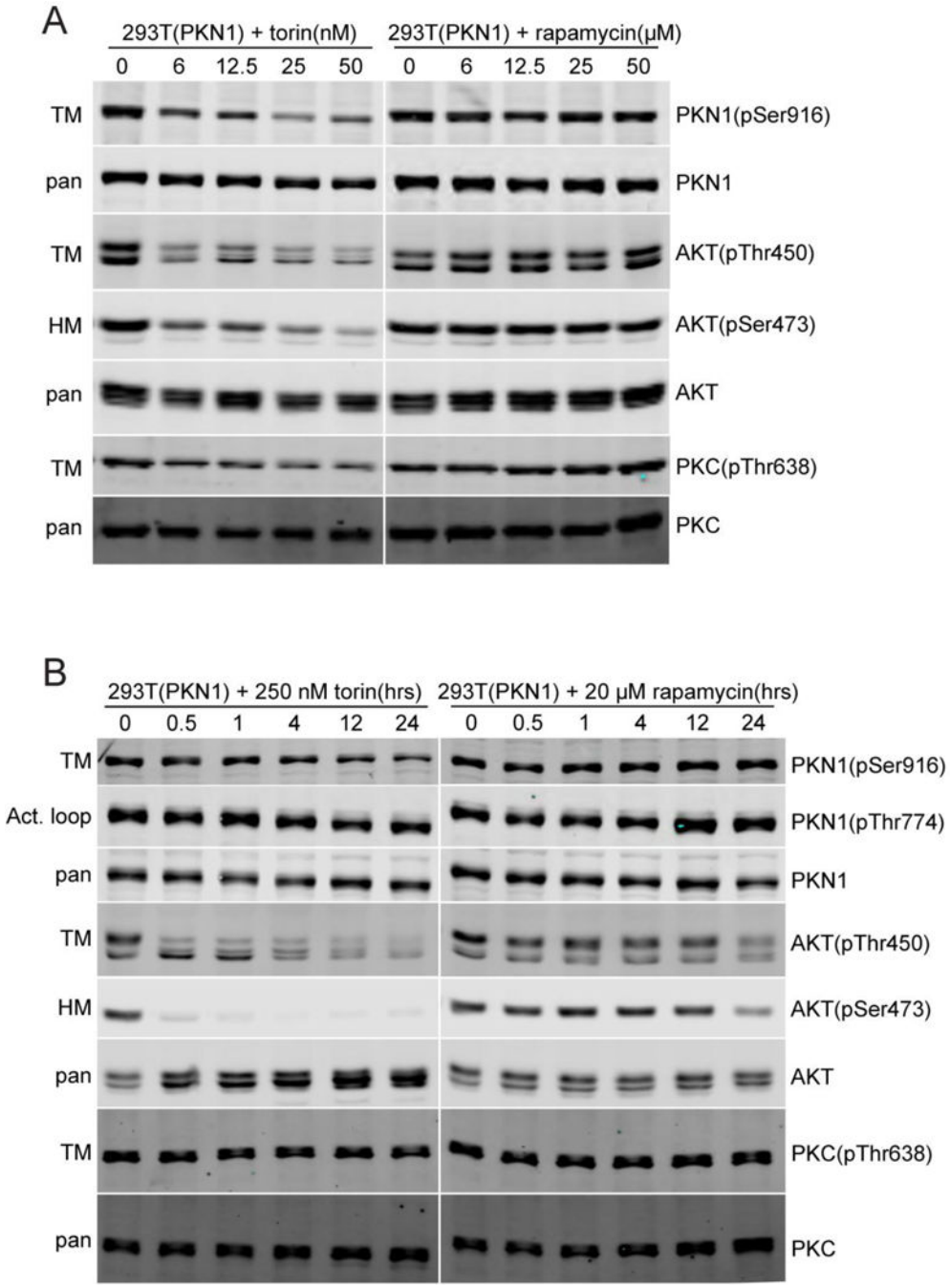

Fig. 3. Torin and rapamycin sensitivity of PKN, AKT, and PKCα

(A) Cells stably transduced with WT PKN1 were treated with a range of torin and rapamycin concentrations for 24 hrs, and analyzed by using pan- and phosphosite-specific antibodies. (B) Cells were treated with torin and rapamycin during a time course up to 24 hrs and subsequently analyzed by using pan- and phosphosite-specific antibodies.

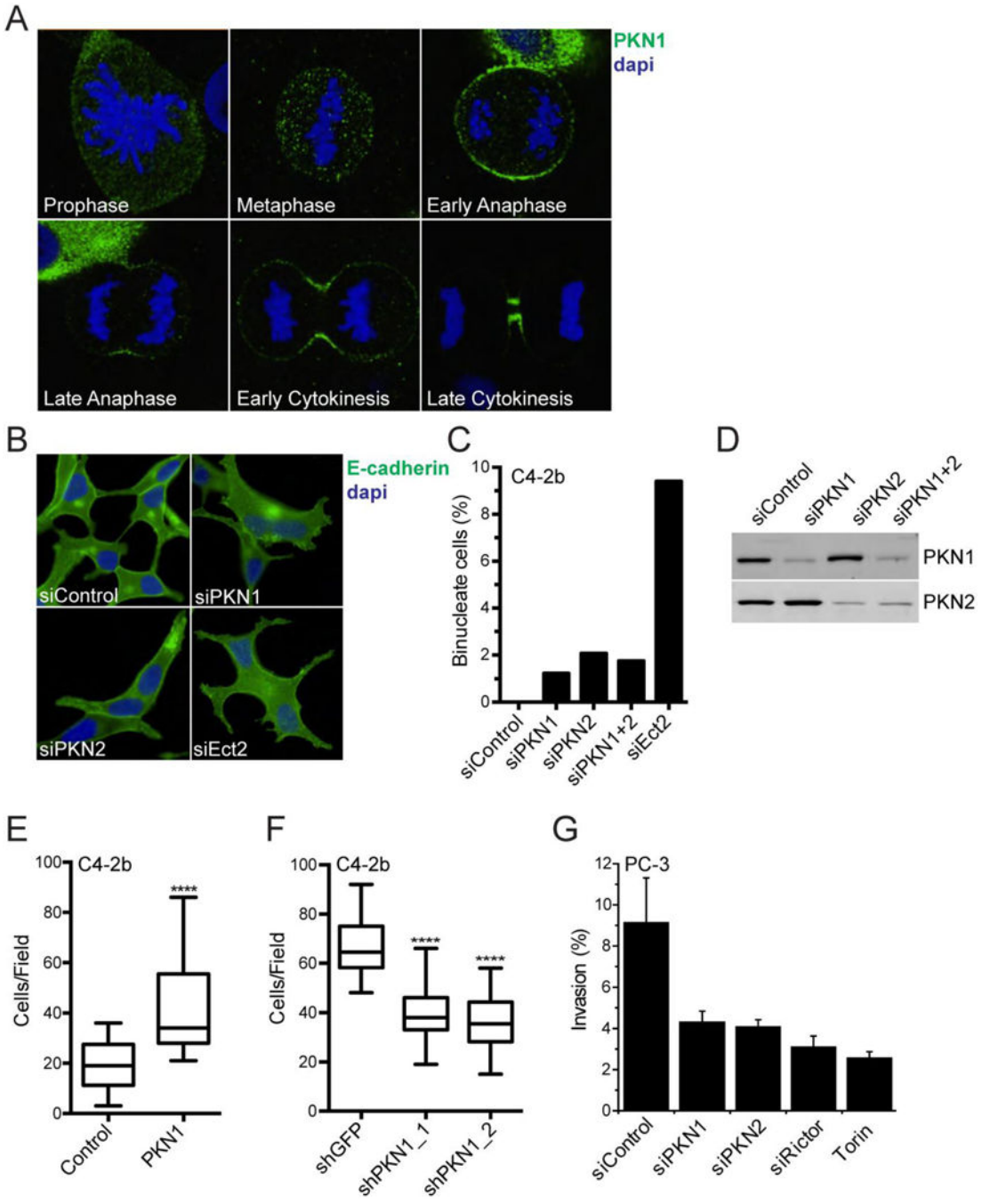

Fig. 4. Cell motility functions of PKN

(A) Localization of Flag-tagged PKN1 (green) at the cleavage furrow during mitosis, imaged by confocal microscopy. (B) Examples of binucleate cells generated in response to depletion of PKN1, PKN2, and Ect2 (positive control), indicative of cytokinesis failure. (C) Quantification of cytokinesis failure data as a consequence of PKN1 and PKN2 depletion. (D) Expression levels (immunoblotting) of PKN1 and PKN2 after siRNA depletion. (E) Stable C4-2b cell lines showing that (E) ectopic expression and (F) knockdown increase and decrease, respectively, cell migration in a Boyden chamber assay (**** p =< 0.0001). (G)

Transient depletion of PKN1, PKN2, and the TORC2 subunit Rictor reduces cell invasion of PC-3 cells to a similar extent as torin treatment.

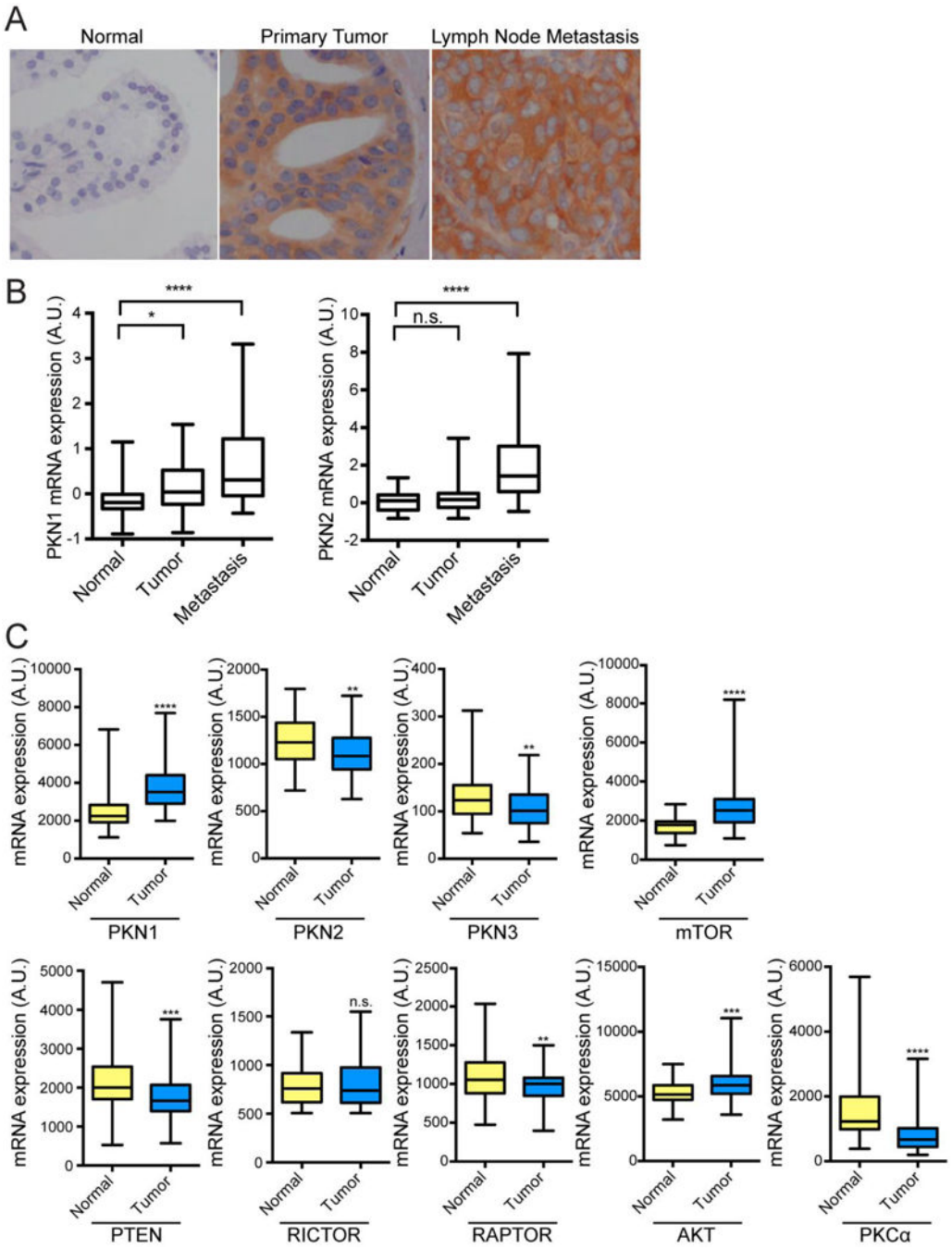

Fig. 5. Analysis of PKN isoform expression in human prostate cancer

(A) Representative IHC showing PKN1 protein levels in normal, primary tumor, and lymph node metastasis. (B) PKN1 and PKN2 expression (using microarray data from [47]) in normal prostate, primary tumor, and metastases. (C) RNA expression (using RNAseq data from TCGA) of PKN1-3 isoforms, PTEN, PKCα, AKT and select mTOR components. ** p =< 0.01 *** p =< 0.001 **** p =< 0.0001

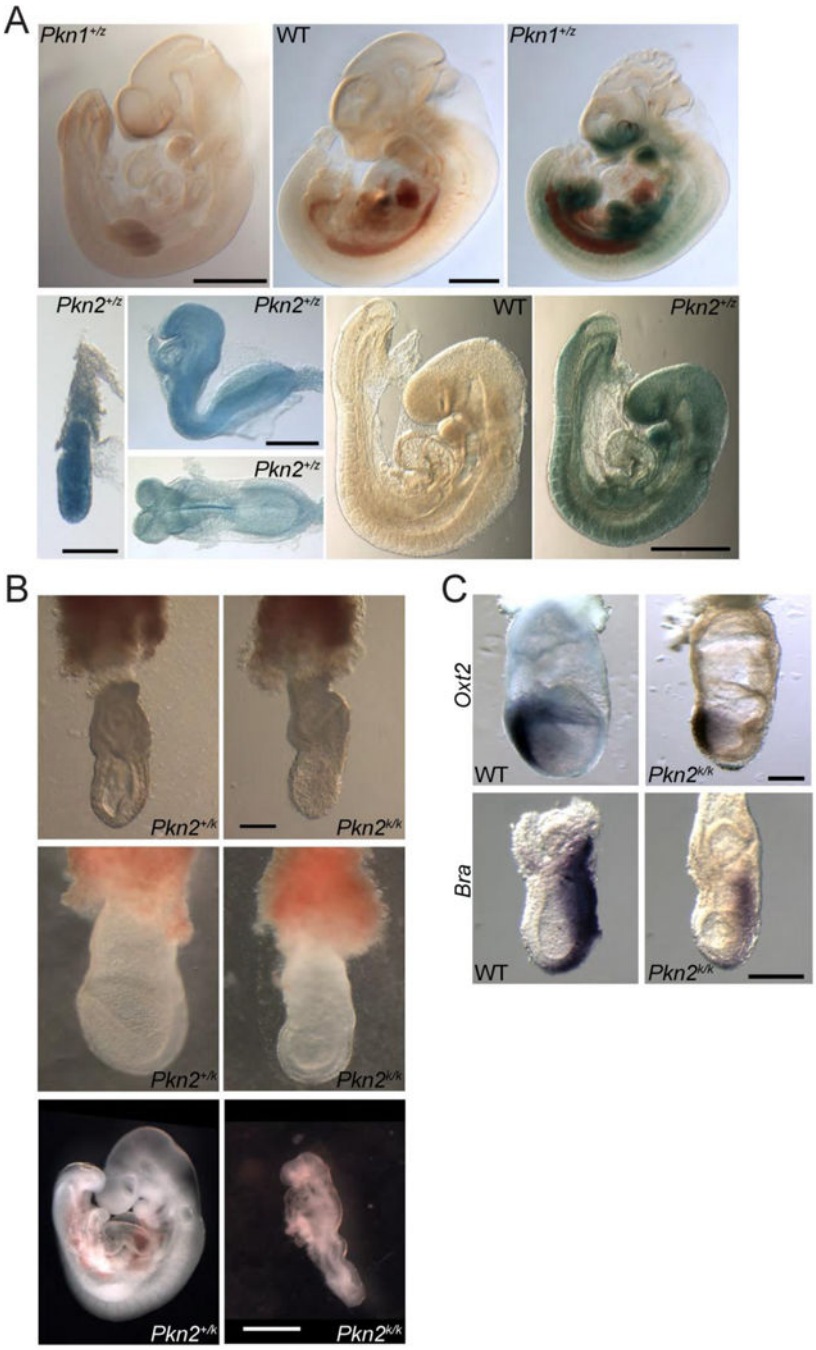

Fig. 6. Pkn2 is required for embryonic development

(A) Embryos from Pkn1 and Pkn2 lacZ reporter mice were stained for β-galactosidase activity, and are shown as whole mount images. Upper row: E10.5, E11.5, E11.5. Scale bars: 1.0mm. Bottom row: E6.5, E8.5 (side and dorsal view), E9.5, E9.5. Scale bars: 0.2mm, 0.5mm, 1.0mm. B) Whole mount images of Pkn2 heterozygotes and homozygous null embryos at E7.0, E7.75 and E9.5. Scale bars 0.2mm (upper four panels), 1.0mm. (C) Whole mount images of wild type and Pkn2 null embryos analyzed by whole mount in situ hybridization for Otx2 (E7.5) and Bra (E7.25) are shown. Scale bars: 0.2mm.

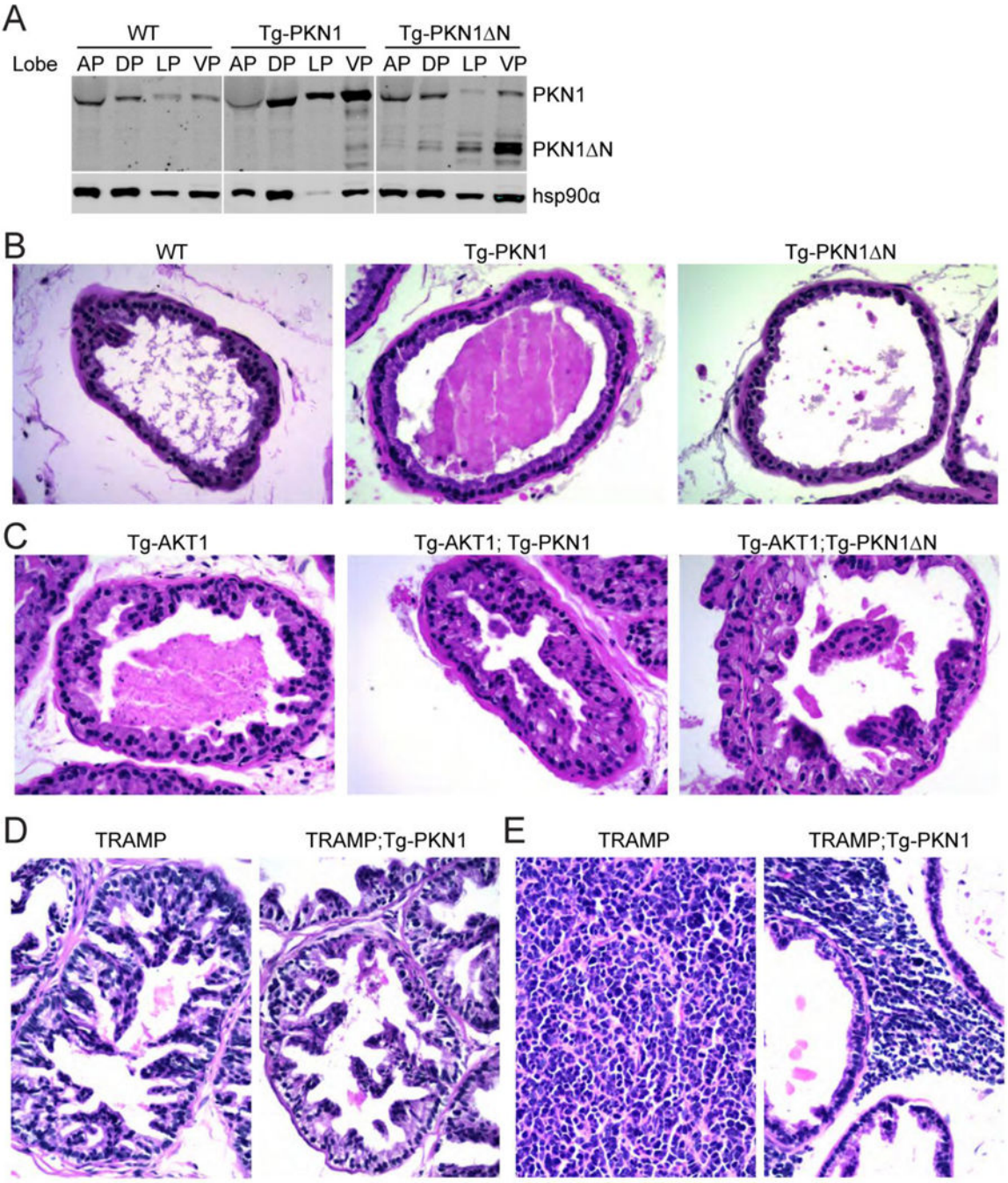

Fig. 7. Analysis of PKN1 overexpression in prostate

(A) Immunoblots showing transgenic expression of full-length (Tg-PKN1) and constitutively active (Tg-PKN1ΔN) proteins in anterior, dorsal, lateral, and ventral lobes (AP, DP, LP, VP). (B–E) H&E stained images of sections through the ventral prostates from mice of the indicated genotypes are shown. The ages of the mice are as follows: WT, 53 weeks; Tg-PKN1, 58 weeks; Tg-PKN1ΔN, 58 weeks; Tg-AKT1, 52 weeks; Tg-AKT1; Tg-PKN1, 41 weeks; Tg-AKT1; Tg-PKN1ΔN, 52 weeks; TRAMP and TRAMP; Tg-PKN1, 16 weeks (showing HGPIN); TRAMP and TRAMP; Tg-PKN1, 17 weeks (showing small cell

carcinoma). All images were captured at 200× magnification. Lower magnification views of the same samples are also provided (Supplemental Fig. 3).

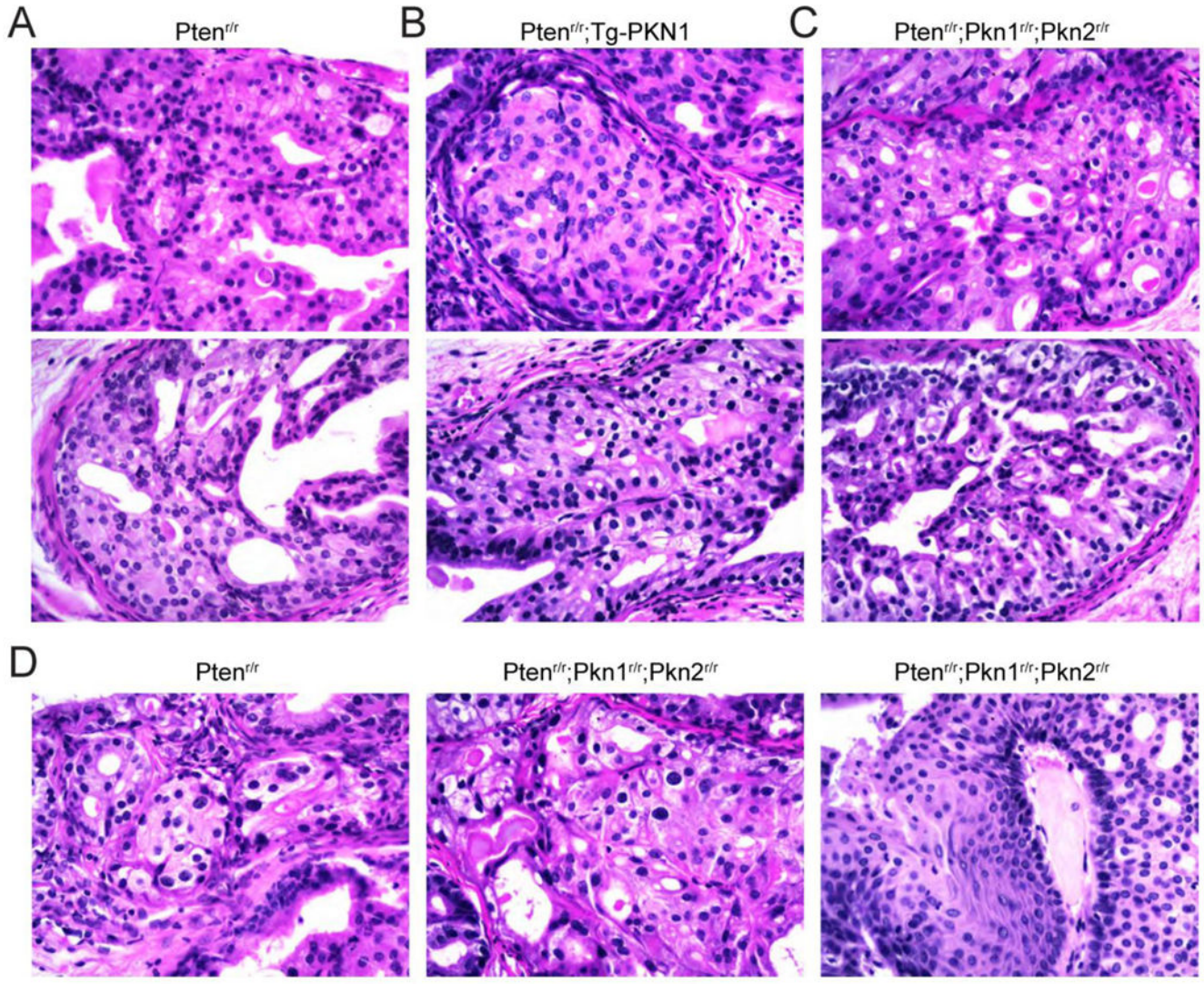

Fig. 8. Analysis of PKNs in Pten null prostate tumors

H&E stained images of sections through the prostates from mice of the indicated genotypes are shown. All images were captured at 200x magnification and are of the ventral prostate, except for the right-most image in panel D, which shows squamous differentiation from the anterior prostate. The ages of the mice (panels A–C) are as follows: $Pten^{r/r}$, 12 and 45 weeks; $Pten^{r/r}$;Tg-PKN1, 12 and 43 weeks; $Pten^{r/r}$;$Pkn1^{r/r}$;$Pkn2^{r/r}$, 26 and 45 weeks. (D) The images of invasive cancer (left and middle) are from 53 week ventral prostates, the squamous differentiation shown to the right is from the anterior prostate of a 53 week animal. Lower magnification views of the same samples are also provided (Supplemental Fig. 4).

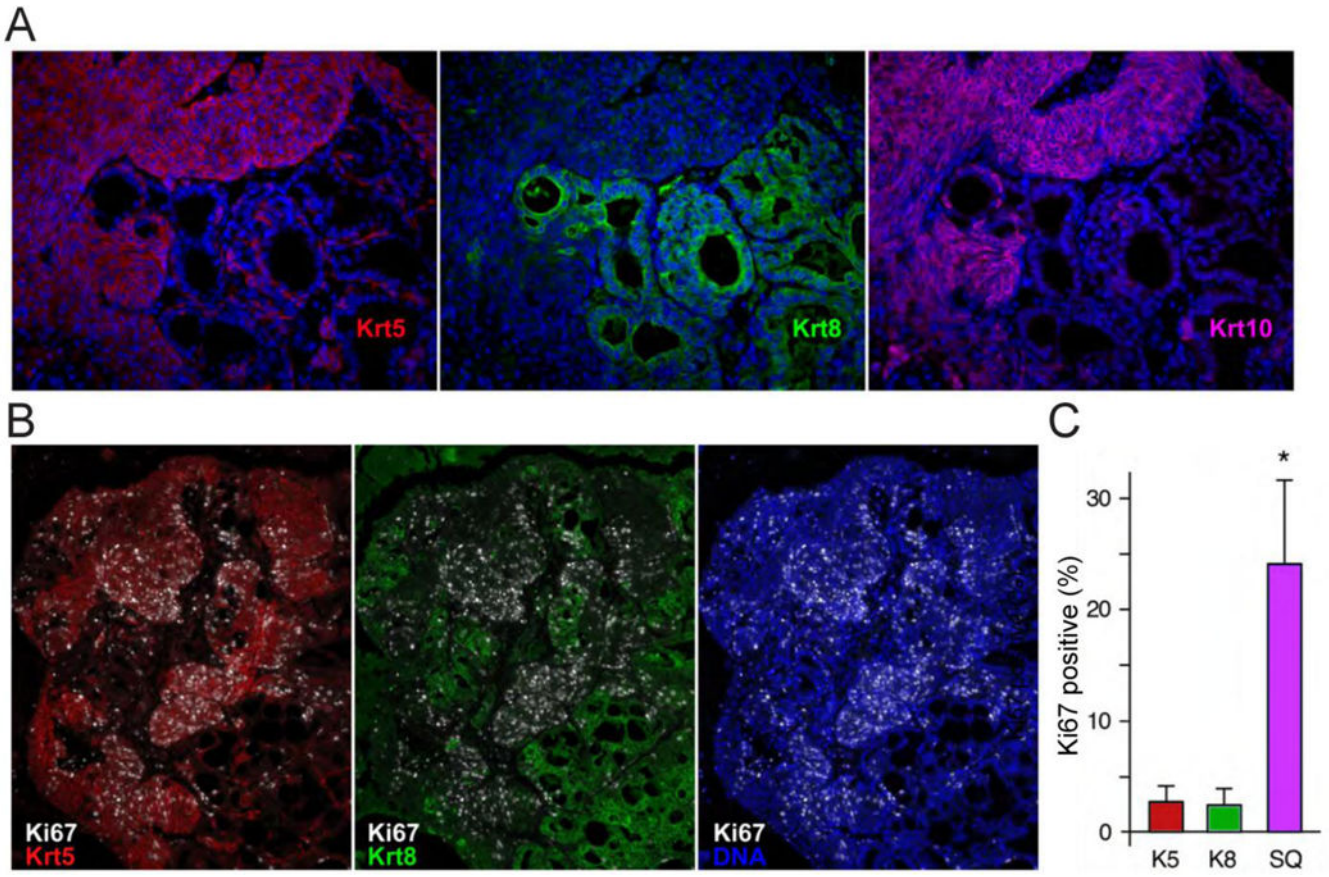

Fig. 9. Squamous differentiation in *Pten$^{r/r}$;Pkn1$^{r/r}$;Pkn2$^{r/r}$* tumors

(A) The anterior prostate of a 53 week *Pten$^{r/r}$;Pkn1$^{r/r}$;Pkn2$^{r/r}$* mouse was analyzed by indirect immunofluorescence for Krt5, Krt8 and Krt10, as indicated. Each individual image is shown overlaid with DAPI staining for nuclei (blue). (B) The anterior prostate of a 53 week *Pten$^{r/r}$;Pkn1$^{r/r}$;Pkn2$^{r/r}$* mouse was analyzed for Krt5, Krt8 and Ki-67, and the merged images for Ki-67 with Krt5, Krt8 or DAPI for DNA are shown. (C) the percentage of Ki-67 positive cells in basal cells surrounding HGPIN (K5), or luminal cells in regions of HGPIN (K8), or of regions of squamous differentiation (SQ) was determined in the prostates from three *Pten$^{r/r}$;Pkn1$^{r/r}$;Pkn2$^{r/r}$* mice. Data is presented as mean plus standard deviation. * $p < 0.05$ compared to K5 and to K8 cells.

Table 1

Genotypes of weaned mice.

Pkn1$^{+/k}$ × Pkn1$^{+/k}$			**(C57BL6/N × 129Sv/J mix)**		
+/+	**+/k**	**k/k**	**total**	**chi sq**	**p-value**
21	32	23	76	2.000	ns
Litters:		15	Average:	5.07	
Pkn1$^{+/k}$ × Pkn1$^{+/k}$			**(C57BL6/N)**		
+/+	+/k	k/k	total	chi sq	p-value
23	30	14	67	3.149	ns
Litters:		14	Average:	4.79	
Pkn2$^{+/k}$ × Pkn2$^{+/k}$			**(C57BL6/N × 129Sv/J mix)**		
+/+	+/k	k/k	total	chi sq	p-value
61	93	0	154	54.97	< 0.001
Litters:		32	Average:	4.81	
Pkn2$^{+/+}$ × Pkn2$^{+/k}$			**(C57BL6/N × 129Sv/J mix)**		
+/+	+/k		total	chi sq	p-value
37	36		73	0.014	ns
Litters:		13	Average:	5.62	
Pkn2$^{+/r}$ × Pkn2$^{+/r}$			**(C57BL6/N × 129Sv/J mix)**		
+/+	+/r	r/r	total	chi sq	p-value
20	21	0	41	19.54	< 0.001
Litters:		7	Average:	5.86	

Table 2

Genotypes of weaned mice from double heterozygous intercrosses.

Pkn1$^{+/k}$;Pkn2$^{+/k}$ × Pkn1$^{+/k}$;Pkn2$^{+/k}$ (C57BL6/N × 129Sv/J mix)												
Pkn1	+/+	+/+	+/+	+/k	+/k	+/k	k/k	k/k	k/k			
Pkn2	+/+	+/k	k/k	+/+	+/k	k/k	+/+	+/k	k/k	total	chi sq	p-value
	6	14	0	17	41	0	4	13	0	95	39.61	< 0.001
Litters:	25	Average:		3.80								

Pkn1 genotype only					
+/+	**+/k**	**k/k**	**total**	**chi sq**	**p-value**
20	58	17	95	4.832	ns

Pkn2 genotype only					
+/+	+/k	k/k	total	chi sq	p-value
27	68	0	95	33.04	p < 0.001

Table 3

Genotypes of embryos from Pkn2 heterozygous intercrosses.

$Pkn2^{+/k}$ × $Pkn2^{+/k}$ (C57BL6/N × 129Sv/J mix)							
	All embryos				**% defective**		
Age	**+/+**	**+/k**	**k/k**	**total**	**+/+**	**+/k**	**k/k**
E7.5	12	57	13	82	8	19	100
E8.5	2	10	2	14	0	10	100
E10.5	12	18	7	37	0	11	100
E12.5	3	17	0	20	0	6	na

Table 4

Prostate phenotypes in the ventral lobe

	Age (weeks)	**8 to 18**			**22 to 31**			**32 to 41**			**44 to 60**			**All (8 to 60)**		
	Phenotype	**NT**[a]	**P**	**C**	**NT**	**P**	**C**	**NT**	**P**	**C**	**NT**	**P**	**C**	**NT**	**P**	**C**
Genotype																
	Tg-PKN1	1						4			7			12		
	Tg-PKN1ΔN				2			4			13			19		
Tg-AKT1			11		1	6	1					5		1	22	1
Tg-AKT1	Tg-PKN1				1				3			3		1	6	
Tg-AKT1	Tg-PKN1ΔN		5			4		1	2			9		1	20	
TRAMP			8	4											8	4
TRAMP	Tg-PKN1		7	1											7	1
TRAMP	Tg-PKN1ΔN		5												5	
$Pten^{r/r}$			20			22	2		15	6		12	6		69	14
$Pten^{r/r}$	Tg-PKN1		14			8			2						24	
$Pten^{r/r}$	Tg-PKN1ΔN		13			9			1			3			26	
$Pten^{r/r}$	$Pkn1^{r/r}$		7						5	1		8	1		20	2
$Pten^{r/r}$	$Pkn1^{r/r}$;$Pkn2^{r/r}$					9			1	2		2	6[b]		12	8

[a] NT: no tumor, P: PIN/HGPIN, C: invasive cancer

[b] 3 mice with extensive squamous differentiation in anterior and dorsolateral prostate; one of these mice had squamous differentiation in the ventral lobe